

Supplement of

Phase state and viscosity of secondary organic aerosols over China simulated by WRF-Chem

Zhiqiang Zhang^{1,2}, Ying Li¹, Haiyan Ran^{1,2}, Junling An¹, Yu Qu¹, Wei Zhou¹, Weiqi Xu¹, Weiwei Hu³, Hongbin Xie⁴, Zifa Wang¹, Yele Sun¹, Manabu Shiraiwa⁵

¹State Key Laboratory of Atmospheric Boundary Layer Physics and Atmospheric Chemistry, Institute of Atmospheric Physics, Chinese Academy of Sciences, Beijing 100029, China

²College of Earth and Planetary Sciences, University of Chinese Academy of Sciences, Beijing 100049, China

³State Key Laboratory of Organic Geochemistry, Guangzhou Institute of Geochemistry, Chinese Academy of Sciences, Guangzhou 510640, China

⁴Key Laboratory of Industrial Ecology and Environmental Engineering (Ministry of Education), School of Environmental Science and Technology, Dalian University of Technology, Dalian 116024, China

⁵Department of Chemistry, University of California, Irvine, Irvine, CA 92697-2025, USA

Correspondence to: Ying Li (liying-iap@mail.iap.ac.cn)

S1. Bulk diffusion coefficient of organic and water molecules within SOA particles.

The diffusion coefficient in the bulk (D_b) is an important parameter determining the mass-transport and mixing rates. We calculate the D_b of organic molecules within SOA particles by the fractional Stokes–Einstein equation (Price et al., 2016; Evoy et al., 2019):

$$D_{b,org} = D_c \left(\frac{\eta_c}{\eta} \right)^\xi \quad (1)$$

where η is the viscosity of SOA particles. The fit parameter ξ is 0.93 (Evoy et al., 2019). η_c is the crossover viscosity at which the Stokes–Einstein equation and the fractional Stokes–Einstein equation predict the same diffusion coefficient. The value of η_c is 10^{-3} Pa s (Evoy et al., 2019). D_c is the crossover diffusion coefficient:

$$D_c = \frac{kT}{6\pi R_{diff} \eta_c} \quad (2)$$

where k is Boltzmann constant (1.38×10^{-23} J K⁻¹), T is the temperature (K), and R_{diff} is the hydrodynamic radius of the diffusing species, with a value of 4×10^{-10} m for organic molecules (Maclean et al., 2021).

The fractional Stokes–Einstein equation is also used to determine the diffusion coefficient of water (Price et al., 2016; Evoy et al., 2019; Evoy et al., 2020):

$$D_{b,H_2O}(RH, T) = D_0(T) \left(\frac{\eta_0(T)}{\eta(RH, T)} \right)^\delta \quad (3)$$

where $D_0(T)$ is the temperature-dependent diffusion coefficient of water molecules in pure water, which can be calculated using the Stokes–Einstein equation (Price et al., 2016). $\eta_0(T)$ is the temperature-dependent viscosity of pure water, obtained from the VTF equation in Maclean et al. (2021): $\log(\eta_0(T)) = A + \frac{B}{T-T_0}$. The values of A , B , and T_0 are -4.28 , 152.87 and 173.06 , respectively, obtained from fitting the temperature-dependent viscosities of water (Hallett, 1963; Crittenden et al., 2012) to the VTF equation. δ is the fractional exponent and can be calculated by Eq. 4:

$$\delta = 1 - \left[A_1 \exp \left(-B_1 \frac{R_{diff}}{R_{matrix}} \right) \right] \quad (4)$$

where A_1 and B_1 are coefficients with values of 0.73 and 1.79 , respectively (Evoy et al., 2020). The radius (R_{diff}) of the diffusing molecule, i.e., the water molecule, is 10^{-10} m. The radius of the matrix molecules (R_{matrix}) is assumed to be 4×10^{-10} m, representing the size of organic molecules (Maclean et al., 2021).

S2. Definitions of model performance statistics.

The mean bias (MB), normalized mean bias (NMB), root mean squared error (RMSE) and index of agreement (IOA) are calculated based on the equations below. P_i represents the simulated data, and O_i represents observed data. N is the number of the data pairs. \bar{O} is the mean value of the observed data:

$$MB = \frac{\sum_{i=1}^N (P_i - O_i)}{N}$$

$$NMB = \frac{\sum_{i=1}^N (P_i - O_i)}{\sum_{i=1}^N O_i} \times 100\%$$

$$RMSE = \sqrt{\frac{\sum_{i=1}^N (P_i - O_i)^2}{(N - 1)}}$$

$$IOA = 1 - \frac{\sum_{i=1}^N (O_i - P_i)^2}{\sum_{i=1}^N (|P_i - \bar{O}| + |O_i - \bar{O}|)^2}$$

Table S1. Physical and chemical options in WRF-Chem used in this study.

Physical/chemical schemes	Options
Advection scheme	Runge-Kutta 3rd order
Cloud microphysics	Lin et al. 1983 (Lin et al., 1983)
Long-wave radiation	RRTM
Short-wave radiation	Goddard
Surface layer	Revised MM5 Monin-Obukhov scheme
Land-surface model	Unified Noah land-surface model
Boundary layer scheme	YSU
Cumulus parameterization	Grell 3D
Photolysis scheme	Madronich F-TUV photolysis
Chemistry option	Updated MOZART-4 mechanism (Emmons et al., 2010)
Aerosol option	MOSAIC (Zaveri et al., 2008)

Table S2. Model performance statistics for simulated hourly mean RH, T , concentrations of $PM_{2.5}$ and $PM_{2.5}$ components at the IAP site.

	Mean (observed)	Mean (simulated)	MB	NMB	RMSE	IOA
RH	40.60 %	29.63 %	-10.97 %	-27.01 %	14.90 %	0.87
T	299.48 K	301.29 K	1.81 K	0.60 %	2.84 K	0.93
$PM_{2.5}$	52.05 $\mu\text{g m}^{-3}$	46.32 $\mu\text{g m}^{-3}$	-3.88 $\mu\text{g m}^{-3}$	-7.45 %	36.40 $\mu\text{g m}^{-3}$	0.64
NH_4^+	5.68 $\mu\text{g m}^{-3}$	3.71 $\mu\text{g m}^{-3}$	-1.90 $\mu\text{g m}^{-3}$	-33.43 %	5.33 $\mu\text{g m}^{-3}$	0.69
NO_3^-	8.71 $\mu\text{g m}^{-3}$	4.27 $\mu\text{g m}^{-3}$	-4.43 $\mu\text{g m}^{-3}$	-50.86 %	11.05 $\mu\text{g m}^{-3}$	0.70
SO_4^{2-}	8.73 $\mu\text{g m}^{-3}$	6.56 $\mu\text{g m}^{-3}$	-1.98 $\mu\text{g m}^{-3}$	-22.70 %	7.01 $\mu\text{g m}^{-3}$	0.70
SOA	11.03 $\mu\text{g m}^{-3}$	5.15 $\mu\text{g m}^{-3}$	-5.88 $\mu\text{g m}^{-3}$	-53.28 %	8.18 $\mu\text{g m}^{-3}$	0.49

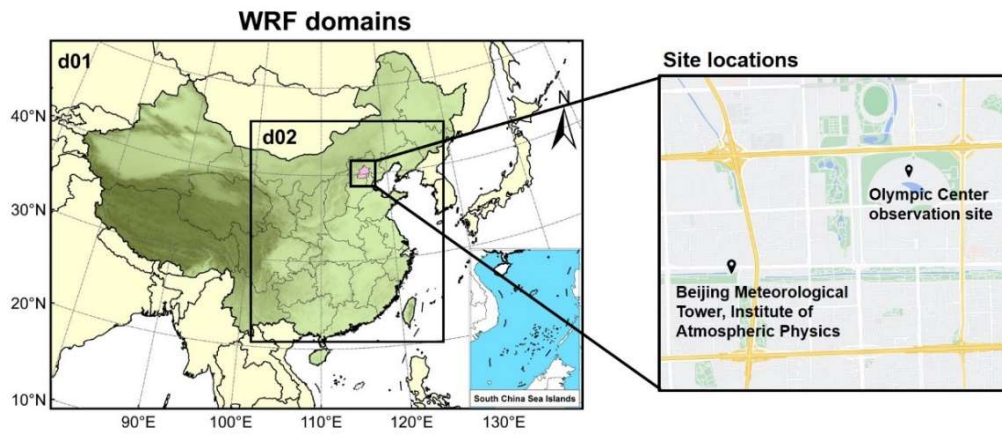


Figure S1. The WRF-Chem model domains and the observation sites. The map of the observation sites is adopted from © Google Maps.

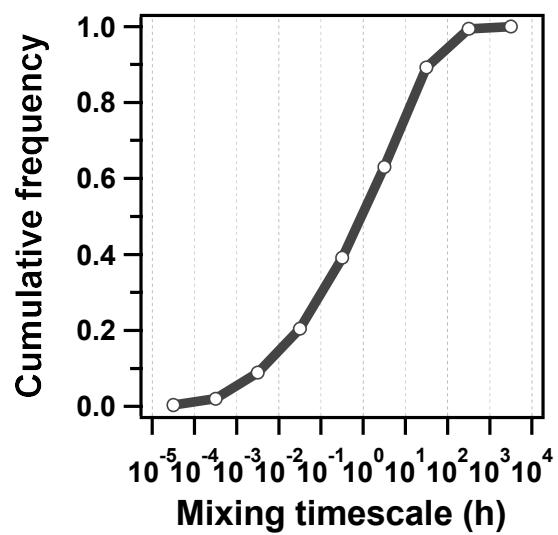


Figure S2. Cumulative distributions of mixing timescales of organic molecules within 200 nm SOA matrix at the IAP site.

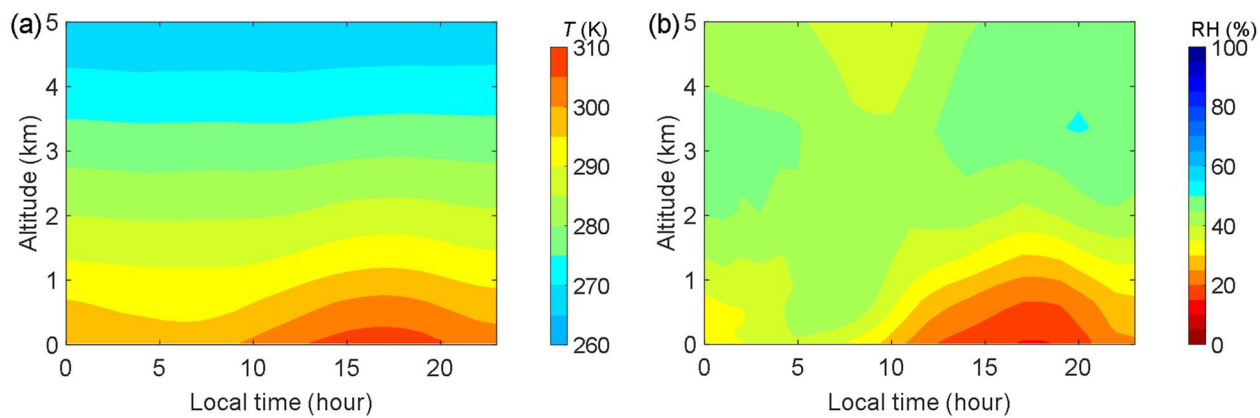


Figure S3. Median diurnal and vertical profiles of WRF-Chem predicted (a) temperature, and (b) relative humidity at the IAP site during May 20 – June 23 in 2018. Note: altitude is approximate and estimated from WRF-Chem pressure layers.

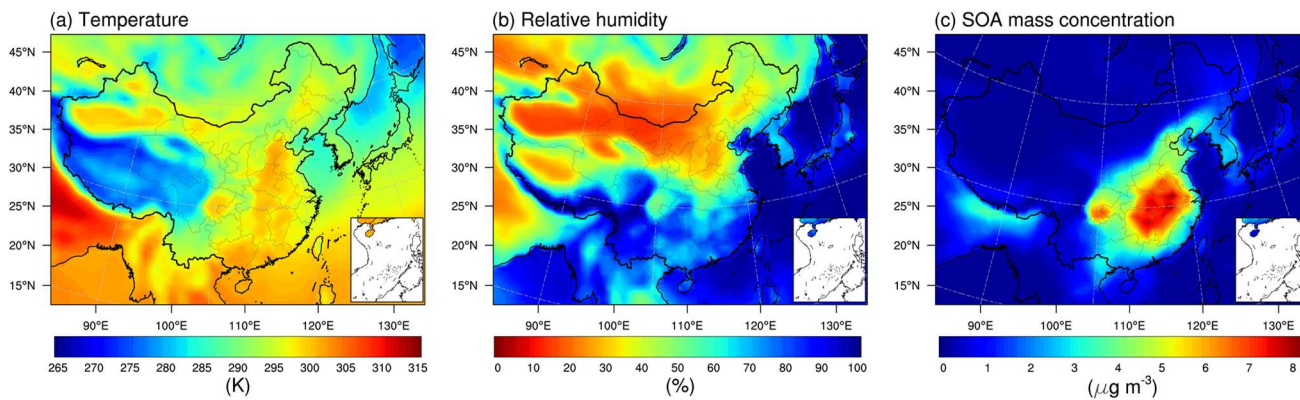


Figure S4. WRF-Chem predicted median surface values of (a) T , (b) RH, and (c) total SOA mass concentrations formed from VOC.

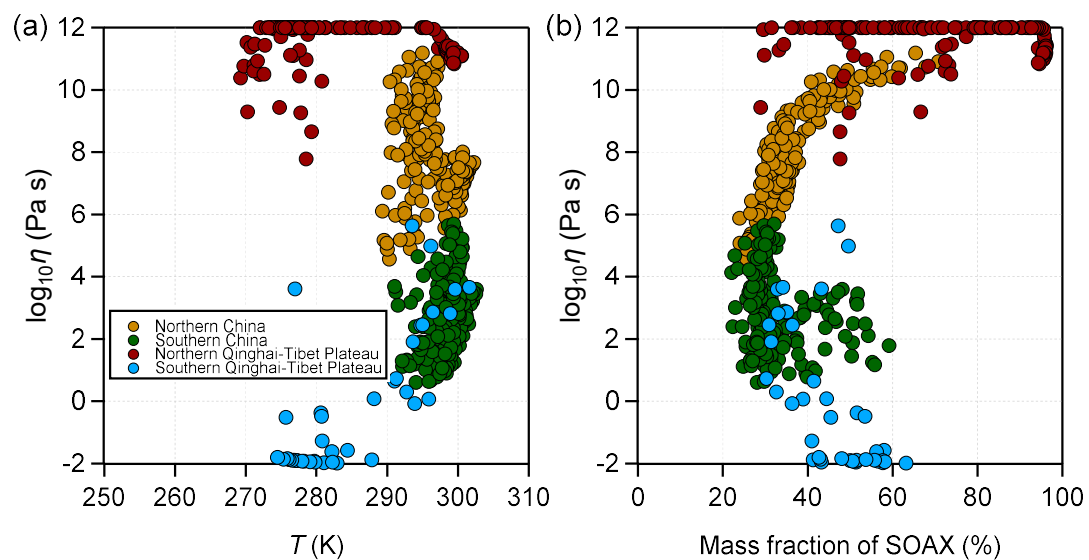


Figure S5. The median values of viscosity as a function of (a) T and (b) the mass fraction of SOAX ($C^* = 0.1 \mu\text{g m}^{-3}$ at 298 K) calculated for selected regions in the northern China, southern China, northern Qinghai-Tibet Plateau, and southern Qinghai-Tibet Plateau as specified by white boxes in panel (a) during May 20 – June 23 in 2018.

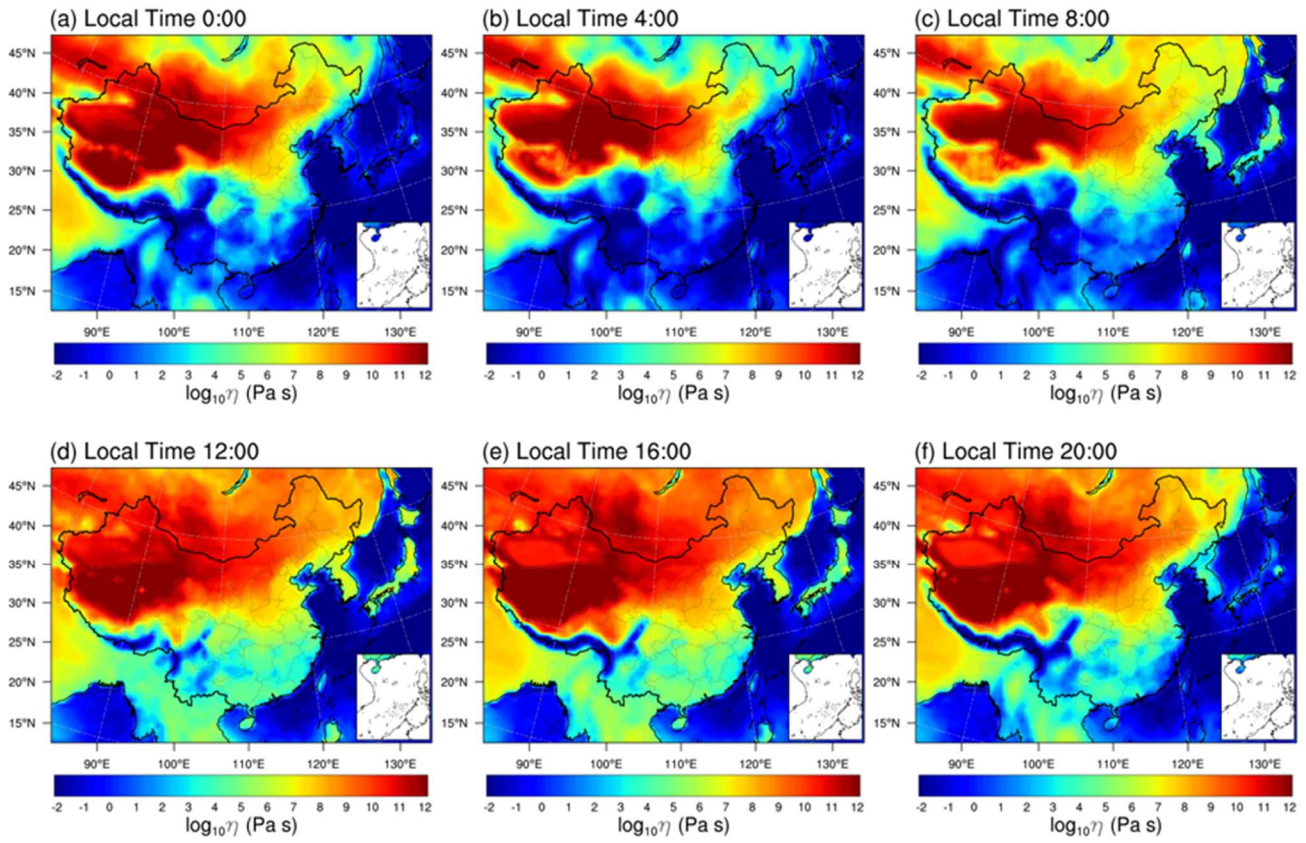


Figure S6. WRF-Chem predicted median surface values of viscosity at local time (hours in Beijing) during May 20 – June 23 in 2018.

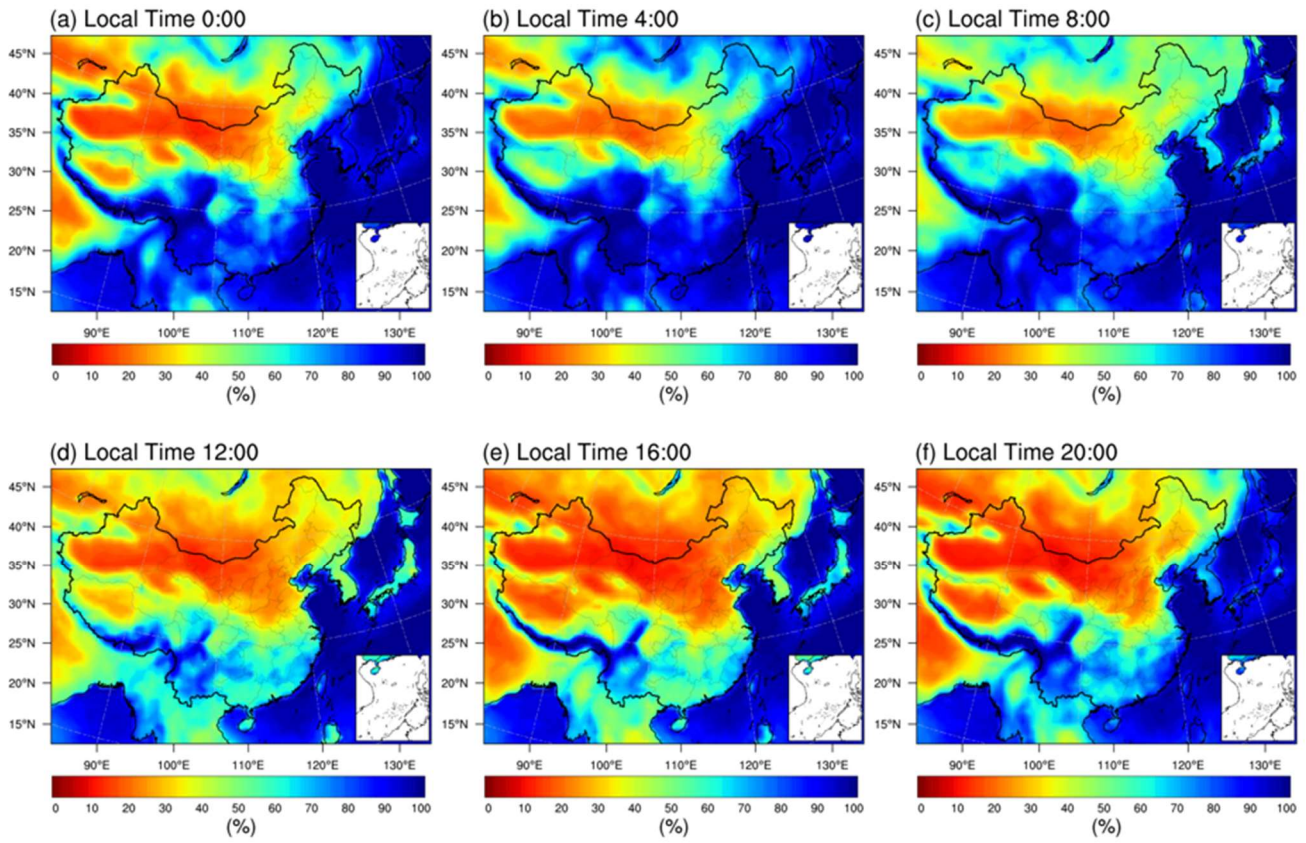


Figure S7. WRF-Chem predicted median surface values of RH at local time (hours in Beijing) during May 20 – June 23 in 2018.

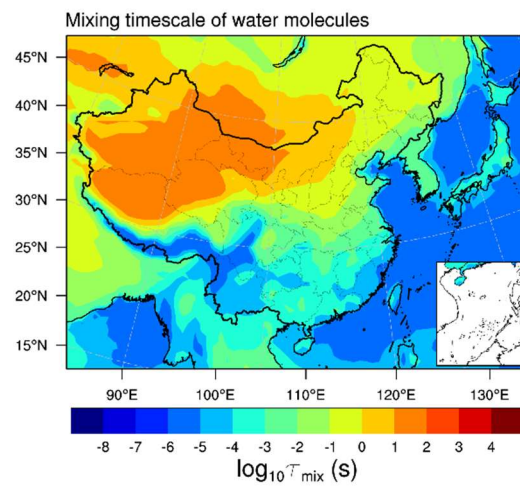


Figure S8. WRF-Chem predicted median surface values of mixing timescales of water molecules in a 200 nm particle during May 20 – June 23 in 2018.

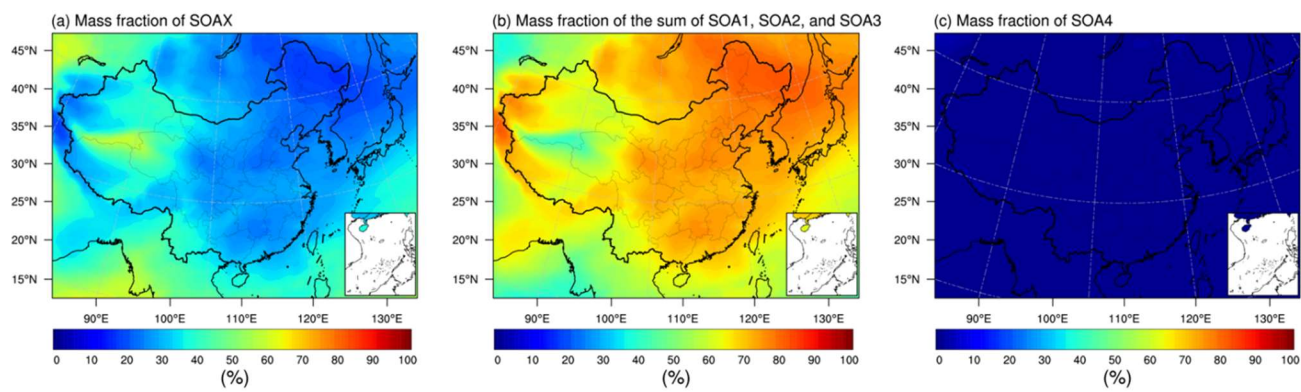


Figure S9. The predicted median values of mass fraction of (a) SOAX, (b) sum of SOA1, SOA2, and SOA3, and (c) SOA4 at 500 hPa during May 20 – June 23 in 2018 simulated in the base case (Table 1). SOAX, SOA1, SOA2, SOA3, and SOA4 represent the SOA with C^* of 0.1, 1, 10, 100, and 1000 $\mu\text{g m}^{-3}$ at 298 K, respectively.

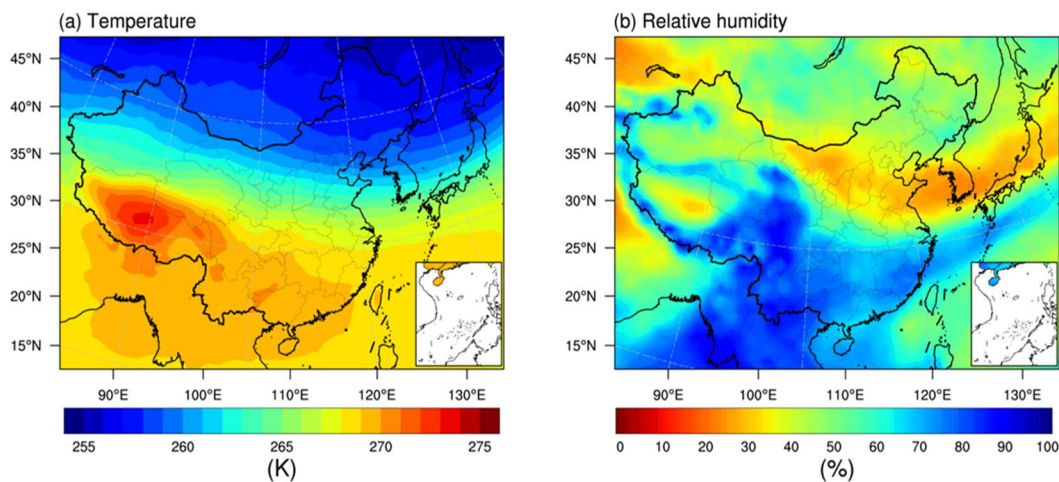


Figure S10. The predicted median values of (a) T and (b) RH at 500 hPa during May 20 – June 23 in 2018 simulated in the base case (Table 1).

References

- Crittenden, J. C., Trussel, R. R., Hand, D. W., Howe, K. J., and Tchobanoglous, G.: MWH's Water Treatment, 2012.
- Emmons, L. K., Walters, S., Hess, P. G., Lamarque, J. F., Pfister, G. G., Fillmore, D., Granier, C., Guenther, A., Kinnison, D., Laepple, T., Orlando, J., Tie, X., Tyndall, G., Wiedinmyer, C., Baughcum, S. L., and Kloster, S.: Description and evaluation of the model for ozone and related chemical tracers, version 4 (MOZART-4), *Geosci. Model Dev.*, 3, 43-67, <https://doi.org/10.5194/gmd-3-43-2010>, 2010.
- Evoy, E., Kamal, S., Patey, G. N., Martin, S. T., and Bertram, A. K.: Unified description of diffusion coefficients from small to large molecules in organic–water mixtures, *J. Phys. Chem. A*, 124, 2301-2308, <https://doi.org/10.1021/acs.jpca.9b11271>, 2020.
- Evoy, E., Maclean, A. M., Rovelli, G., Li, Y., Tsimpidi, A. P., Karydis, V. A., Kamal, S., Lelieveld, J., Shiraiwa, M., Reid, J. P., and Bertram, A. K.: Predictions of diffusion rates of large organic molecules in secondary organic aerosols using the Stokes–Einstein and fractional Stokes–Einstein relations, *Atmos. Chem. Phys.*, 19, 10073-10085, <https://doi.org/10.5194/acp-19-10073-2019>, 2019.
- Hallett, J.: The temperature dependence of the viscosity of supercooled water, *Proc. Phys. Soc.*, 82, 1046-1050, <https://doi.org/10.1088/0370-1328/82/6/326>, 1963.
- Lin, Y.-L., Farley, R. D., and Orville, H. D.: Bulk parameterization of the snow field in a cloud model, *J. Appl. Meteorol. Clim.*, 22, 1065-1092, [https://doi.org/10.1175/1520-0450\(1983\)022%3C1065:BPOTSF%3E2.0.CO;2](https://doi.org/10.1175/1520-0450(1983)022%3C1065:BPOTSF%3E2.0.CO;2), 1983.
- Maclean, A. M., Li, Y., Crescenzo, G. V., Smith, N. R., Karydis, V. A., Tsimpidi, A. P., Butenhoff, C. L., Faiola, C. L., Lelieveld, J., Nizkorodov, S. A., Shiraiwa, M., and Bertram, A. K.: Global distribution of the phase state and mixing times within secondary organic aerosol particles in the troposphere based on room-temperature viscosity measurements, *ACS Earth Space Chem.*, 5, 3458-3473, <https://doi.org/10.1021/acsearthspacechem.1c00296>, 2021.
- Price, H. C., Mattsson, J., and Murray, B. J.: Sucrose diffusion in aqueous solution, *Phys. Chem. Chem. Phys.*, 18, 19207-19216, <https://doi.org/10.1039/C6CP03238A>, 2016.
- Zaveri, R. A., Easter, R. C., Fast, J. D., and Peters, L. K.: Model for Simulating Aerosol Interactions and Chemistry (MOSAIC), *J. Geophys. Res.: Atmos.*, 113, <https://doi.org/10.1029/2007JD008782>, 2008.